OPEN ACCESS
CellPress

Cell Reports
Article

LIF Mediates Proinvasive Activation of Stromal Fibroblasts in Cancer

Jean Albrengues,[1] Isabelle Bourget,[1] Catherine Pons,[1] Vincent Butet,[2] Paul Hofman,[3] Sophie Tartare-Deckert,[4] Chloe C. Feral,[1] Guerrino Meneguzzi,[1] and Cedric Gaggioli[1,*]
[1]INSERM, U1081, CNRS, UMR7284, Institute for Research on Cancer and Aging, Nice (IRCAN), University of Nice Sophia Antipolis, Medical School, 28 Avenue Valombrose, F-06107 Nice, France
[2]Pathological Anatomy and Cytology Laboratory, 270 Avenue Sainte-Marguerite, F-06200 Nice, France
[3]Laboratory of Clinical and Experimental Pathology and Hospital-Integrated Tumor Biobank, Pasteur Hospital, F-06002 Nice, France
[4]INSERM, U1065, Mediterranean Centre for Molecular Medicine (C3M), University of Nice Sophia Antipolis, F-06204 Nice, France
*Correspondence: gaggioli@unice.fr
http://dx.doi.org/10.1016/j.celrep.2014.04.036

SUMMARY

Signaling crosstalk between tumor cells and fibroblasts confers proinvasive properties to the tumor microenvironment. Here, we identify leukemia inhibitory factor (LIF) as a tumor promoter that mediates proinvasive activation of stromal fibroblasts independent of alpha-smooth muscle actin (α-SMA) expression. We demonstrate that a pulse of transforming growth factor β (TGF-β) establishes stable proinvasive fibroblast activation by inducing LIF production in both fibroblasts and tumor cells. In fibroblasts, LIF mediates TGF-β-dependent actomyosin contractility and extracellular matrix remodeling, which results in collective carcinoma cell invasion in vitro and in vivo. Accordingly, carcinomas from multiple origins and melanomas display strong LIF upregulation, which correlates with dense collagen fiber organization, cancer cell collective invasion, and poor clinical outcome. Blockade of JAK activity by Ruxolitinib (JAK inhibitor) counteracts fibroblast-dependent carcinoma cell invasion in vitro and in vivo. These findings establish LIF as a proinvasive fibroblast producer independent of α-SMA and may open novel therapeutic perspectives for patients with aggressive primary tumors.

INTRODUCTION

Malignant evolution of solid cancers relies on complex cell-to-cell interactions sustained by a broad network of physical and chemical mediators that constitutes the tumor microenvironment (Hanahan and Weinberg, 2011). Such a cellular network involves both tumor and nontumor cells embedded in a modified extracellular matrix (ECM) rich in growth factors, chemokines, and cytokines that supports cancer cell growth and invasive spreading (Calvo and Sahai, 2011). Carcinoma-associated fibroblasts (CAFs) are the most representative noncancer cells within the tumor microenvironment (Calvo et al., 2013; Joyce and Pollard, 2009), and their presence is associated with poor clinical prognosis (Boyd et al., 2007; Lin et al., 2012; Navab et al., 2011; Shi et al., 2012; Takahashi et al., 2011). It is clear that under the influence of bioactive molecules within the tumor stroma, resident fibroblasts are activated and promote tumorigenesis (Beacham and Cukierman, 2005; Bhowmick et al., 2004b; De Wever et al., 2008; Kalluri and Zeisberg, 2006; Olumi et al., 1999). Indeed, CAFs can support tumor initiation (Trimboli et al., 2009), inflammation (Erez et al., 2010), and angiogenesis (Orimo et al., 2005). CAFs are also responsible for proinvasive ECM remodeling and track formation leading to collective carcinoma cell invasion (Gaggioli et al., 2007). Therefore, understanding how cancer cells induce a fibroblast-dependent proinvasive tumor microenvironment may provide key issues for prognosis and treatment of patients with solid cancers.

Inflammation is a hallmark of cancer progression (Coussens and Werb, 2002; Hanahan and Weinberg, 2011). It is established that paracrine secretion of multiples molecules, including transforming growth factor β (TGF-β), growth factors, and proinflammatory molecules such as interleukin-6 (IL-6) family cytokines, by cancer cells, promotes tumorigenesis (Calvo and Sahai, 2011; Lederle et al., 2011). TGF-β family cytokines are known to drive myofibroblast activation during wound healing and cancer progression (Desmoulière et al., 1993; Phan, 2008), but the role of stroma-specific TGF-β-dependent signaling during cancer invasion remains, however, unclear. Indeed, specific stromal deletion of TGF-β-receptor (TGF-βr) II in mice promotes invasive tumorigenesis (Achyut et al., 2013; Bhowmick et al., 2004a; Franco et al., 2011). Similarly, pharmacological inhibition of TGF-βr-I in a mouse model of chemically induced carcinoma development represses papilloma progression toward development of aggressive carcinoma (Mordasky Markell et al., 2010).

The role of TGF-β-dependent signaling in cancer promotion is multifaceted, and targeting TGF-β signaling in patients has been so far deceiving (Connolly et al., 2012). Here, we identify the proinflammatory cytokine LIF as a proinvasive tumor microenvironment promoter, and we show that high-level expression of LIF correlates with poor clinical outcome for patients with grade I and II head and neck and lung carcinomas. Produced

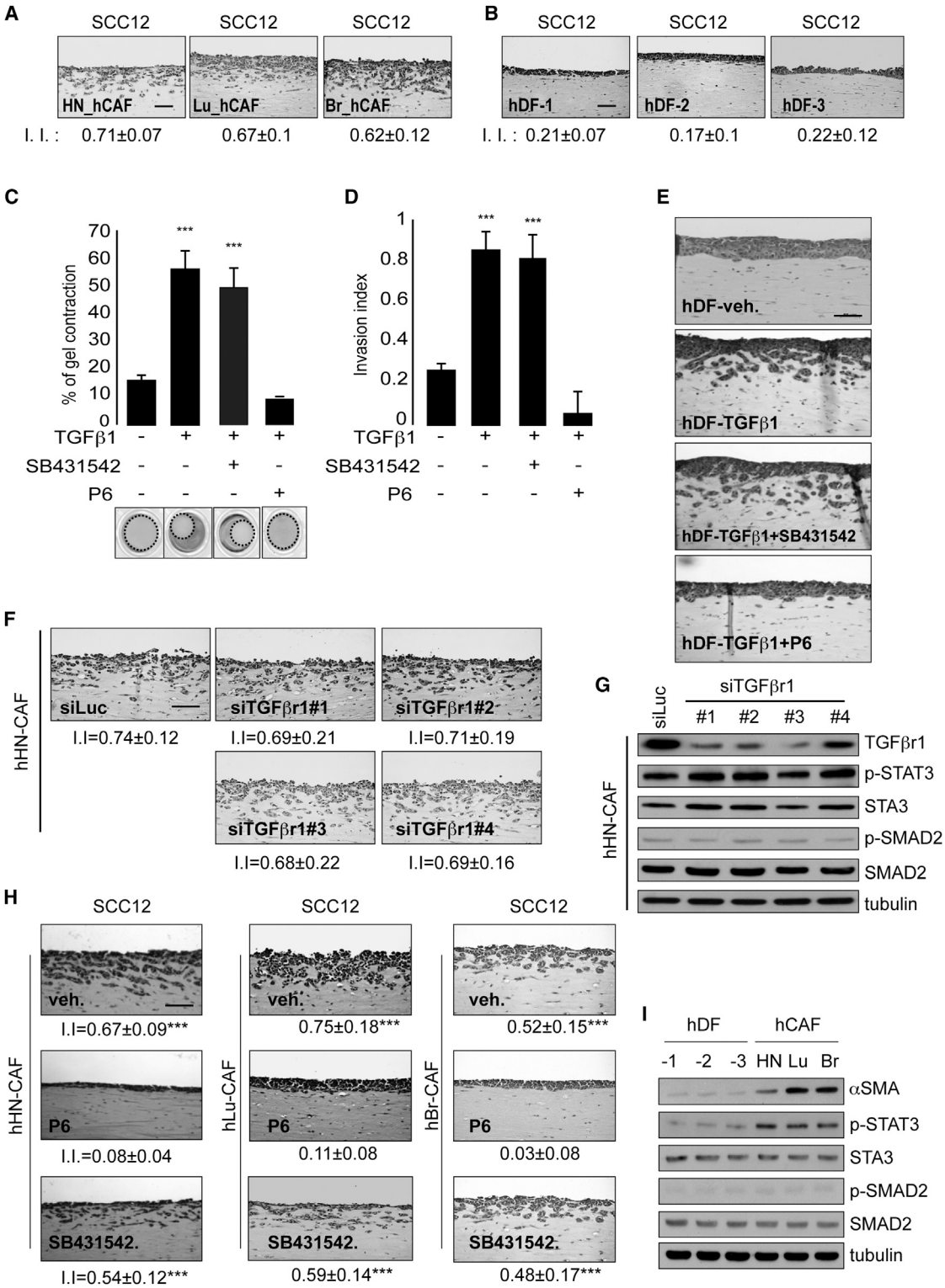

Figure 1. TGF-β1 Signaling Initiates and JAK Signaling Sustains Proinvasive Fibroblast Property

(A) Representative images of hematoxylin and eosin (H&E) coloration of paraffin-embedded sections of SCC12 cells in response to three distinct hCAF, head and neck (HN), lung (lu), and breast (Br) cell cultures. I.I., invasion index; n = 3; mean ± SD; ***p < 0.001. Scale bar, 100 μm.

(B) H&E coloration of paraffin-embedded sections of SCC12 cells in response to three hDF cell cultures (hDF-1, -2, -3). I.I., invasion index; n = 3; mean ± SD; ***p < 0.001. Scale bar, 100 μm.

(legend continued on next page)

by tumor cells from multiple origin and fibroblasts upon TGF-β1 stimulation, LIF drives fibroblast-dependent proinvasive tumor microenvironment through regulation of actomyosin contractility independent of alpha-smooth muscle actin (α-SMA) expression. Inhibition of JAK kinase activity by the JAK1/2 FDA-approved Ruxolitinib inhibitor blocks induction and maintenance of proinvasive ECM remodeling with consequent inhibition of cancer cell invasion in vitro and in vivo. These findings disclose potential therapeutic opportunities for patients with advanced cancer.

RESULTS

TGF-β1 Confers Proinvasive Properties to Fibroblasts via a JAK1/STAT3-Dependent Signaling Pathway

Human CAFs isolated from head and neck squamous cell (hHN-CAF), lung (hLu-CAF), or breast (hBr-CAF) carcinoma (Table S1) support proinvasive ECM remodeling, as visualized in vitro by their capacity to contract collagen gels (Figure S1A, black bars) and human carcinoma SCC12 cell invasion (Figure 1A), whereas human primary dermal fibroblasts (hDFs) displayed no appreciable contractile phenotype (Figure S1B, black bars) and failed to induce SCC12 cell collective invasion (Figure 1B). Because the TGF-β cytokines, including TGF-β1, 2, and 3, are known to promote myofibroblast activation during wound healing and tumorigenesis (Desmoulière et al., 1993; Phan, 2008), we speculated that the TGF-β/SMAD signaling pathway might be responsible of the hDF conversion into contractile and proinvasive human carcinoma-associated fibroblasts (hCAF)-like cells. Indeed, in hDF, transient pulse of TGF-β1 stimulation induced both contractility (Figures 1C and S1B) and proinvasive properties (Figures 1D and 1E), but TGF-β-dependent signaling is dispensable for maintenance of the proinvasive phenotype in CAFs and activated hDF (Figures 1C–1H, S1C, and S1D; SB431542, LY364947, and A83-01 inhibitors). In agreement with the notion that JAK kinase activity is needed for proinvasive track formation by hHN-CAF (Sanz-Moreno et al., 2011), we found that hLu-CAF and hBr-CAF cells required JAK signaling to sustain their proinvasive potential (Figures 1H and S1A–S1D; P6, Ruxolitinib, Cyt387, and Tofacinib inhibitors). The possible contribution of the JAK kinase signaling to the proinvasive properties of TGF-β1-activated hDF was thus assessed using specific inhibitors. Similar to hCAF cells, TGF-β1-activated fibroblasts were found to rely on JAK but not on TGF-βr-I signaling to promote matrix contraction (Figures 1C, S1A, and S1B) and SCC12 cell collective invasion (Figures 1D, 1E, and 1H). This confirmed that TGF-β signaling is sufficient to promote but not necessary to sustain the proinvasive activity, a function that relies on JAK kinase signaling. Further, according with previous results (Sanz-Moreno et al., 2011), and similar to hHN-CAF, the TGF-β1-activated hDF resulted to rely on JAK1/STAT3-specific signaling to acquire ability for proinvasion track formation within the ECM (Figures S1E–S1G). Accordingly, hCAF cells expressing the α-SMA marker displayed an enhanced endogenous activity of STAT3 (Figure 1I), which correlated with their endogenous levels of collagen gel contractility (Figures S1A and S1B, black histograms). Taken together, these data suggest that a transient stimulation of hDF by TGF-β1 is sufficient to induce the proinvasive phenotype in hCAF, which is then sustained by a JAK1/STAT3-dependent signaling.

LIF Supports TGF-β1-Dependent Actomyosin Contractility toward a Proinvasive Tumor Microenvironment

We next investigated the molecular mechanisms that govern TGF-β1-dependent JAK/STAT signaling activation. Stimulation of hDF by TGF-β1 induces phosphorylation of STAT3 and SMAD2 transcription factors. However, whereas SMAD2 activation occurs within 10 min, STAT3 activation is delayed up to 1 hr (Figure 2A), which suggests involvement of distinct molecular mechanisms. Because IL-6 cytokines are known to support JAK/STAT activation (Kishimoto et al., 1995), transcription of the *IL6* cytokine gene family members in TGF-β1-stimulated hDF was thus assessed by quantitative real-time PCR, that disclosed a 100-fold increase of *LIF* and 5-fold increase of *IL6* mRNA steady-state levels (Figure 2B). The respective role of these two cytokines was investigated using specific blocking antibodies, which identified LIF as the major cytokine mediating STAT3 phosphorylation upon TGF-β1 stimulation (Figure 2C). Interestingly, LIF was detected in hDF cell culture medium 1 hr after TGF-β1 stimulation, with a 24 hr peak of 200 pg/ml (Figure 2D), and, as expected, the pan-JAK inhibitor P6 blocked the STAT3 phosphorylation induced by TGF-β1 (Figure 2C). The involvement of LIF signaling in the TGF-β1-mediated STAT3 phosphorylation was confirmed by small interfering RNA (siRNA)-mediated knockdown of GP130-IL6ST. Indeed, silencing of the common subunit receptor of the IL-6 family cytokine GP130-IL6ST hampered STAT3 activation by TGF-β1 without affecting SMAD2 activation (Figure S2A). These results support the conclusion that in hDF TGF-β1 relies on a LIF/GP130-IL6ST/JAK1 signaling cascade to induce STAT3

(C) Quantification of matrix contraction by hDF stimulated by TGF-β1 (2 ng/ml) for 7 days and subsequently treated by TGF-βr-I inhibitor (SB431542) and pan-JAK inhibitor (P6) (n = 3 in triplicates; mean ± SD; ***p < 0.001). Bottom panel shows scanned images of the contracted gel.
(D) Quantification of SCC12 cell organotypic invasion assay index (experiments shown in E) induced by TGF-β1-activated hDF for 7 days and subsequently treated with TGF-βr-I inhibitor (SB431542) or JAK kinase inhibitor (P6) (n = 3; mean ± SD; ***p < 0.001).
(E) H&E coloration of paraffin-embedded sections of organotypic invasion assays quantified in (D). Scale bar, 100 μm.
(F) H&E coloration of paraffin-embedded sections of SCC12 cell invasion assays induced by hHN-CAF following TGF-βr1 protein depletion. siLuc is used as RNAi control transfection. Scale bar, 100 μm. (I.I. = Invasion index; n = 3; mean ± SD; ***p < 0.001.)
(G) Immunoblotting of TGF-βr1, STAT3, p-STAT3, SMAD2, p-SMAD2, and tubulin after RNAi-mediated TGF-βr1 depletion. siLuc as control of RNAi transfection.
(H) H&E coloration of paraffin-embedded sections of SCC12 cells in response to three hCAF (HN, Lu, and Br) in the presence of P6, SB431542, or control (Veh). Scale bar, 100 μm. (I.I., invasion index; n = 3; mean ± SD; ***p < 0.001.)
(I) Immunoblotting of α-SMA, p-STAT3, and p-SMAD2 in three hDF (hDPF-1, -2, -3) and three hCAF (HN-CAF, Lu-CAF, and Br-CAF) cells. Immunoblot of STAT3, SMAD2, and tubulin shown as controls.

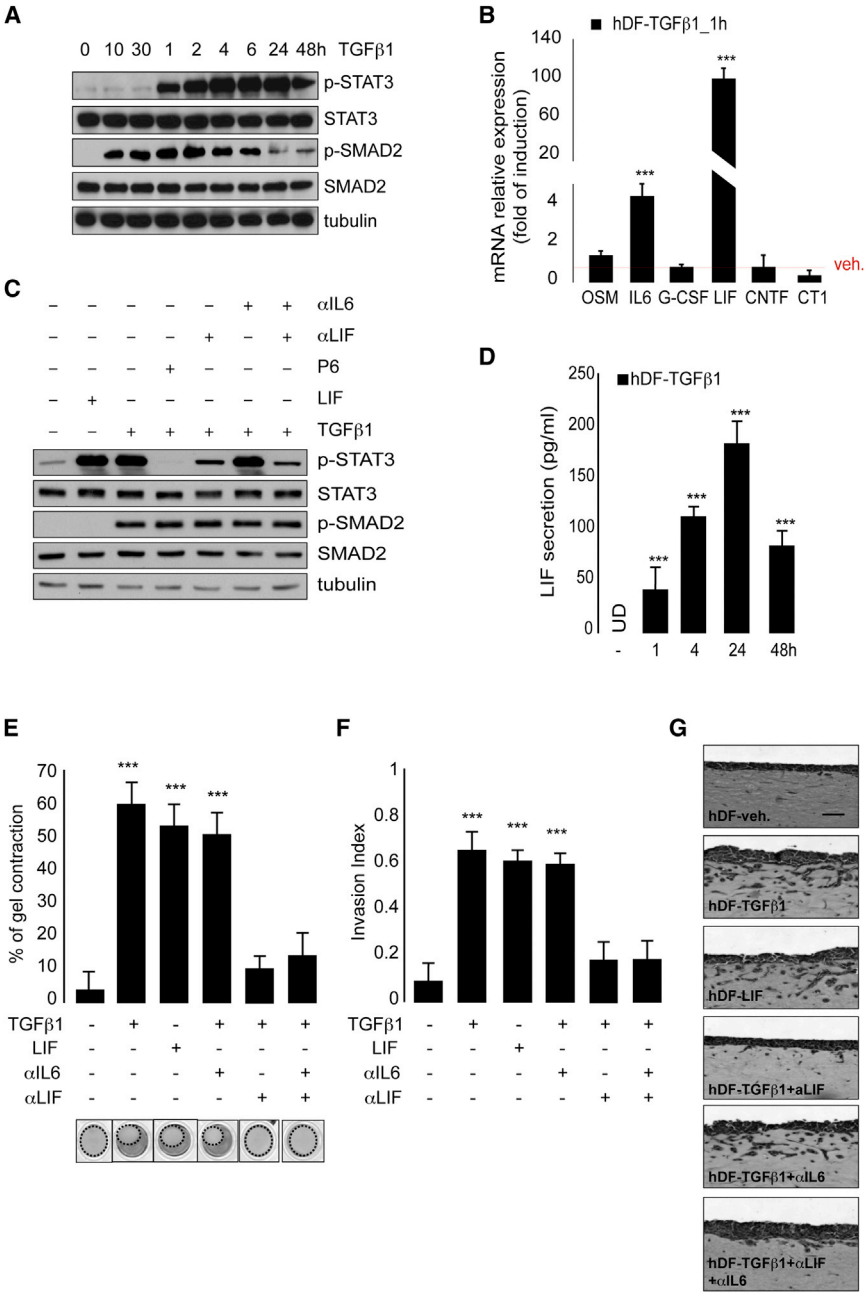

Figure 2. LIF Mediates TGF-β1-Dependent Proinvasive Fibroblast Activation

(A) Immunoblot of p-STAT3 and p-SMAD2 following TGF-β1 time course stimulation of hDF. Immunoblot of STAT3, SMAD2, and tubulin as controls.

(B) Quantification of mRNA level relative to the control (Veh) of OSM, IL-6, G-CSF, LIF, CNTF, and CT1 1 hr after TGF-β1-stimulation. (n = 3 in duplicates; mean ± SD; ***p < 0.001.)

(C) Immunoblotting of p-STAT3 and p-SMAD2 after LIF or TGF-β1 stimulation in presence or absence of P6 or LIF and/or IL-6 blocking antibodies in hDF. Immunoblot of STAT3, SMAD2, and tubulin as control.

(D) ELISA quantification of LIF secreted in TGF-β1-stimulated hDF culture media. (UD, undetectable; n = 3 in duplicates; mean ± SD; ***p < 0.001.)

(E) Quantification of matrix remodeling by hDF stimulated by TGF-β1 or LIF in the presence or absence of LIF (αLIF) and IL-6 (αIL6) blocking antibodies for 7 days. (n = 3 in triplicates; mean ± SD; ***p < 0.001.) Bottom panel shows scanned images of the contracted gel.

(F) Quantification of SCC12 cell organotypic invasion index induced by hDF stimulated by TGF-β1 or LIF in the presence of LIF and/or IL-6 blocking antibodies (n = 3; mean ± SD, ***p < 0.001).

(G) H&E coloration of paraffin-embedded sections of the SCC12 invasion assays quantified in (F). Scale bar, 100 μm.

activation and suggest that hDF just stimulated by LIF may promote onset of a proinvasive microenvironment. According with this idea, both matrix remodeling (Figure 2E) and SCC12 cell collective invasion were observed with hrLIF-stimulated hDF (Figures 2F and 2G); further, LIF sequestration using a specific blocking anti-LIF antibody counteracted the action of TGF-β1 (Figures 2E–2G). In light of these observations, we deduced that TGF-β1 specifically activates the proinvasive properties of hDF via the LIF/GP130-IL6ST/JAK1 signaling axis. Because JAK1 and ROCK cooperate to control actomyosin contractility in hHN-CAF, which results in proinvasive tracks formation within the ECM (Sanz-Moreno et al., 2011), the potential role of the RhoA/ROCK-dependent signaling pathway in LIF-mediated proinvasive fibroblast activation was investigated. siRNA-mediated knockdown of RhoA expression or pharmacological inhibition of Rho-kinase (ROCK) activity resulted in blockade of both TGF-β1 and LIF-dependent proinvasive hDF activity (Figures S2B and S2C). Long-term stimulation of both TGF-β and LIF cytokines also upregulated RhoA small GTPase and myosin light chain 2 (MLC2) proteins, leading to an increase in MLC2 phosphorylation at ser19, which attests for an increased activity (Figure S2D). Finally, forced expression of an active form of ROCK (ROCK-ER) (Croft and Olson, 2006) following 4-hydroxytamoxifen (4OHT) treatment was sufficient to induce hDF contractility (Figure S2E), proinvasive capacity (Figures S2Fa and b), and MLC2 phosphorylation (Figure S2G) and also rescued the inhibitory effect of P6 or anti-LIF antibody treatments under TGF-β1 stimulation (Figures S2Fc and d). Taken together, these data suggest that hDF activation by TGF-β1 or LIF requires actomyosin contractility, which is regulated by JAK signaling. In conclusion, in fibroblasts, the proinflammatory cytokine LIF mediates TGF-β1-dependent actomyosin contractility and proinvasive ECM remodeling.

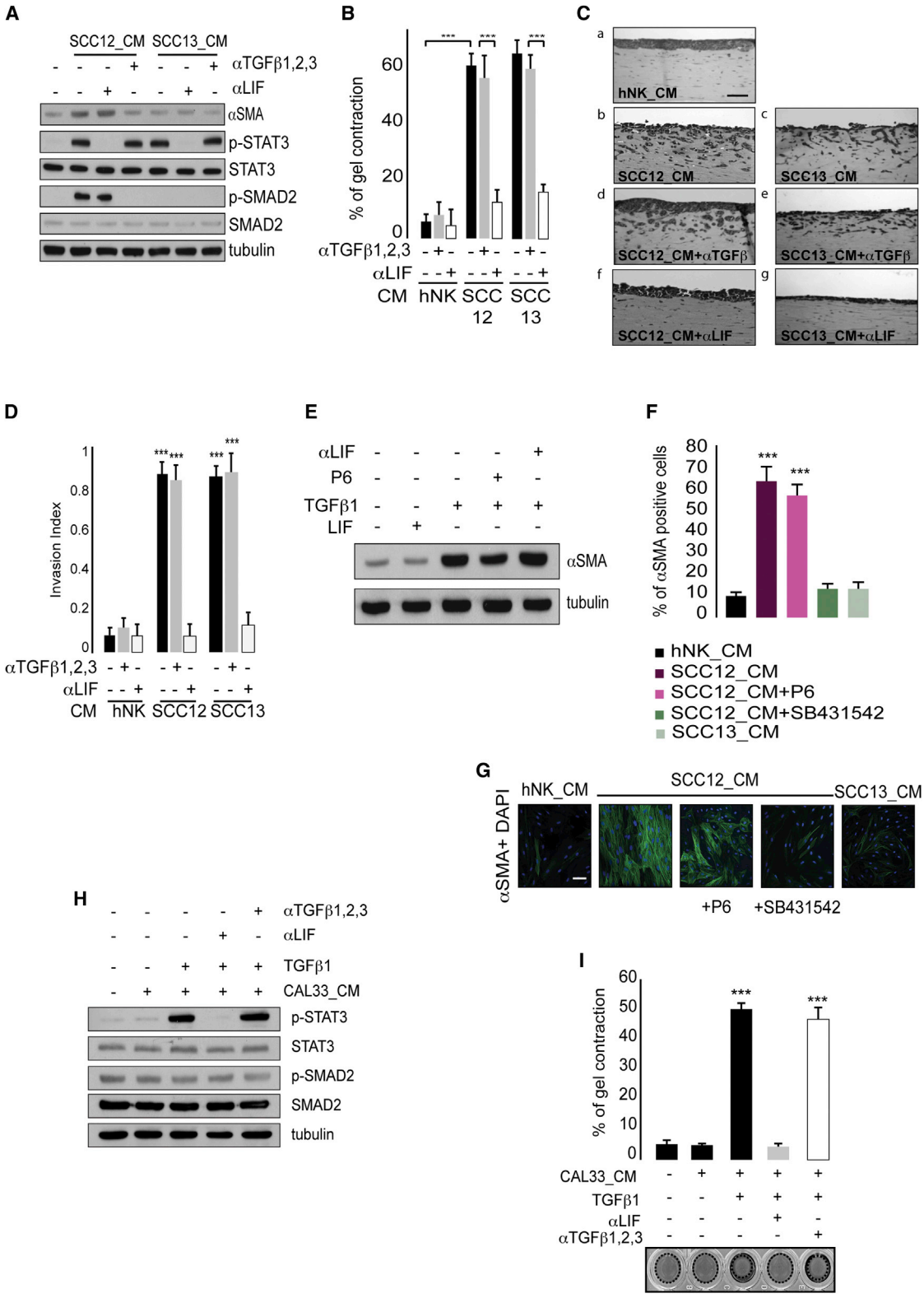

Figure 3. LIF Mediates TGF-β1-Dependent Actomyosin Contractility Independent of α-SMA Expression

(A) Immunoblotting of α-SMA, p-STAT3, and p-SMAD2 in hDF long-term stimulated (7 days) using SCC12 and SCC13 CM in the absence or presence of LIF and TGF-β1, -2, -3 blocking antibodies. Immunoblotting of total STAT3, SMAD2, and tubulin shown as control.

(legend continued on next page)

LIF Mediates Fibroblast Activation to Promote Invasive Tumor Microenvironment Independent of α-SMA Expression

Within the tumor microenvironment, secretion of growth factors and cytokines (García-Tuñón et al., 2008; Sriuranpong et al., 2003; Szepietowski et al., 2004; Wysoczynski et al., 2007) by cancer cells is thought to activate the adjacent fibroblasts (Calvo and Sahai, 2011; De Wever et al., 2008; Kalluri and Zeisberg, 2006; Phan, 2008). In our experiments, conditioned media (CM) by SCC12 human carcinoma cell promoted both paracrine STAT3 and SMAD2 activation in fibroblasts, whereas SCC13 cell CM activated STAT3 but not SMAD2 phosphorylation (Figure 3A and Table 1). SCC12 and SCC13 cells were further used to investigate the role of TGF-β/SMAD2 and JAK/STAT3 signaling in tumor cell-dependent proinvasive fibroblast activation and expression of α-SMA protein, the latter being a CAF hallmark activated in hDF by the TGF-β signaling (Desmoulière et al., 1993). Both SCC12 and SCC13 CM promoted fibroblasts-dependent collagen gel contraction and collective invasion of SCC12 cells in vitro (Figures 3B, 3Ca–c, 3D, and S3Aa–c) compared with human normal keratinocytes (hNK) CM as negative control (Figures 3Ca, 3D, S3Aa, and S3B). Blockade of paracrine SMAD2 phosphorylation by an anti-TGF-β antibody to SCC12 CM (Figure 3A) had no effect on proinvasive fibroblast activation (Figures 3Cd,e and 3D), whereas addition of either a specific LIF-blocking antibody (Figures 3A, 3Cf and g, and 3D) or the ROCK inhibitor Y27632 (Figures S3Ad and e and S3B) completely abrogated the action of SCC12 and SCC13 CM. Importantly, α-SMA expression, which depends on TGF-β signaling independently of LIF (Figure 3E), was induced by the SCC12 CM (Figures 3A, 3F, and 3G) but not by the SCC13 CM that activated fibroblasts STAT3 only through LIF secretion (Figures 3A, 3F, and 3G). Both SCC12 and SCC13 CM increased MLC2 protein levels and activity, which specifically depended on LIF secretion (Figure S3C). Thus, in hDF, α-SMA upregulation appears to be uncoupled from acquisition of proinvasive capacity, which, on the contrary, is conferred by the "tumoral" LIF that relies on the crosstalk between JAK/STAT and Rho/ROCK/MLC2 signaling pathways. This hypothesis was verified using the CAL33 cell line, whose CM neither contains LIF nor activates hDF proinvasiveness (Figures 3H, 3I, and S3G; Table 1). Indeed, hDF maintained in CM from CAL33 cells engineered to secrete transgenic hLIF (CAL33-LIF; Figure S3D) showed paracrine activation of matrix remodeling (Figure S3E) and STAT3 phosphorylation (Figure S3F). Also, CAL33-LIF CM induced proinvasive fibroblast conversion that was blocked by addition of either a LIF-specific blocking antibody (Figures S3G and S3H) or the Y27632 ROCK inhibitor (Figures S3I and S3J). Because TGF-β was found to stimulate LIF production in hDF, the capacity of TGF-β-dependent signaling to induce LIF secretion by tumor cells was investigated. Stimulation of CAL33 cells by TGF-β1 resulted in LIF secretion, which promoted both STAT3 activation and contractility in hDF (Figures 3H and 3I). Moreover, addition of a LIF-specific blocking antibody to CM of TGF-β1-stimulated CAL33 resulted in complete inhibition of both STAT3 phosphorylation and matrix remodeling (Figures 3H and 3I). We thus concluded that in human tumors, including skin, head and neck, lung, colon, and breast carcinomas as well as melanomas (Table 1), LIF signaling mediates onset of a proinvasive microenvironment by proinvasive fibroblast activation and actomyosin contractility regulation independent of α-SMA expression.

LIF and JAK Kinase Signaling Drive Invasive Tumor Microenvironment in Breast Carcinomas

The role of LIF production by tumor cells during invasive tumor ECM remodeling was then investigated in vivo. LIF secretion was first monitored in a panel of mouse breast carcinoma cell lines spanning from a poorly tumorigenic to a highly invasive phenotype (Aslakson and Miller, 1992; Yang et al., 2004). High in vitro LIF secretion levels were found with 4T07, 410.4, and 4T1 invasive cancer cells, whereas LIF secretion was low in 67NR noninvasive tumor cells (Figure 4A). In vitro, LIF production by mouse tumor cells correlated with potential to induce contractility in mouse fibroblasts (Figure S4A). LIF low-producer (67NR) and LIF high-producer (410.4) mouse breast carcinoma cells were then injected into mammary fat pads of syngeneic BALB/c female mice. Thirty days after implantation, mice were sacrificed, and primary tumors were analyzed by immunohistochemistry. Strong LIF-specific staining was exclusively observed in the primary tumor mass generated by 410.4 cells (Figures 4Ba and b) that correlated with sustained STAT3 activation in 410.4 but not in 67NR tumors both in vivo (Figures 4Bc and d) and in vitro (Figure 4C), which identify in LIF secreted by the tumor cells the major cytokine driving STAT3 activation in fibroblasts. In vitro stimulation of mouse dermal fibroblasts by CM of 410.4 cells resulted in SMAD2 activation and α-SMA

(B) Quantification of gel contraction by hDF cells cultured in the presence of SCC12 or SCC13 CM in control (black histograms) depleted for either TGF-β1, -2, -3 (αTGF-β; gray histograms) or for LIF (αLIF; white histogram) at 10 μg/ml of blocking antibodies. (n = 3 in triplicates; mean ± SD. ***p < 0.001 and **p < 0.01.)
(C) H&E coloration of paraffin-embedded sections of SCC12 cell organotypic invasion assays in the presence of hDF cells cultured in CM. hNK (a), SCC12 (b), and SCC13 (c) depleted for either TGF-β1, -2, -3 (αTGF-β; d and e) or LIF (αLIF; f and g). Scale bar, 100 μm.
(D) Quantification of SCC12 cell invasion index from (C) (n = 3; mean ± SD; ***p < 0.001).
(E) Immunoblot of α-SMA protein expression in hDF stimulated by either TGF-β1 or LIF in presence or absence of P6 inhibitor and LIF blocking antibody after 7 days. Tubulin shown as control.
(F) Histograms represent quantification of α-SMA-positive hDF 5 days after stimulation by tumor cell conditioned media (n = 3; mean ± SD; ***p < 0.001).
(G) Representative confocal merged images of α-SMA and DAPI staining in hDF stimulated by SCC12 and SCC13 CM in presence or absence of P6 and SB431542 inhibitors. Scale bar, 50 μm.
(H) Immunoblotting of p-STAT3 and p-SMAD2 in hDF after short-term stimulation by control (veh.) or CAL33 CM in absence or presence of LIF or TGF-β blocking antibodies. CAL33 were stimulated by TGF-β1 during 48 hr, and conditioned media was collected 24 hr after multiple washes in 0.5% serum DMEM. Immunoblotting of total STAT3, SMAD2, and tubulin shown as controls.
(I) Quantification of gel contraction by hDF grown in the presence of control (veh.) or TGF-β1-stimulated CAL33 conditioned media (CM) in control (black histograms) depleted for LIF (αLIF; gray) or TGF-β1, -2, -3 (αTGF-β1, -2, -3; white) at 10 μg/ml of blocking antibodies (n = 3 in triplicates; mean ± SD. ***p < 0.001).

Table 1. LIF Production by Carcinoma Cells from Different Origins Mediates Proinvasive Fibroblast Activation

Cancer Cell Lines	STAT3-Y705 in Fibroblasts[a]	SMAD2-S465/467 in Fibroblasts[a]	Fibroblasts Contractile and Proinvasive Phenotype[b]							LIF ELISA (pg/ml)[c]
			Veh	SB 431542	P6	Ruxo	αIL6 (10 μg/ml)	αLIF (10 μg/ml)[d]	αTGF-β (10 μg/ml)	
Human OSCC										
hPK	–	–	–	–	–	–	–	–	–	UD
SCC12	++	++	+	+	–	–	+	–	+	129.05 ± 12.4
SCC13	++	–	+	+	–	–	+	–	+	276.64 ± 18.6
SCC25	+	++	+	+	–	–	+	–	+	48.11 ± 3.05
CAL27	++	++	+	+	–	–	+	– (50)	+	400.06 ± 22.12
CAL33	–	–	–	–	–	–	–	–	–	UD
CAL60	++	+	+	+	–	–	+	–	+	77.33 ± 4.24
CAL166	++	+	+	+	–	–	+	–	+	84.14 ± 6.32
Detroit562	+	++	+	+	–	–	+	–	+	102.97 ± 8.43
Human Colon Carcinoma										
LS174	++	+	+	+	–	–	+	–	+	185.29 ± 9.87
Human Lung Carcinoma										
A549	++	+	+	+	–	–	+	–	+	95.11 ± 6.49
Human Breast Carcinoma										
MDA-MB-231	+++	++	+	+	–	–	+/–	+/–	+	216.79 ± 15.32
MDA-MB-468	++	++	+	+	–	–	+	+	+	64.34 ± 4.54
Human Melanoma										
A375P	++	+	+	+	–	–	+	–	+	276.69 ± 18.12
A375M2	+++	++	+	+	–	–	+	– (50)	+	545.38 ± 32.87
Mel501	–	–	–	–	–	–	–	–	–	UD
Sbcl2	–	–	–	–	–	–	ND	–	ND	6.78 ± 2.32
WM35	++	–	+	+	–	–	ND	–	ND	403 ± 30.32
WM278	+	+	+	+	–	–	ND	–	ND	98.07 ± 7.3
WM793	+	+	+	+	–	–	ND	–	ND	251.13 ± 13
Mel1205	++	ND	+	+	–	–	ND	–	ND	198.46 ± 65
Human Engineered Cell Line										
CAL33_mock	–	–	–	–	–	–	–	–	–	UD
CAL33_LIF	+++	–	+	+	–	–	+	+(50)	+	1,176.03 ± 86.5
Murine Breast Carcinoma										
67NR	–	–	–	ND		–	ND	–	ND	14.5 ± 20.51
4T07	++	+/–	+	ND		–	ND	–	ND	603.09 ± 49.54
410.4	++	++	+	ND		–	ND	–	ND	927.35 ± 17.00
4T1	++	+	+	ND		–	ND	–	ND	1,523.25 ± 162.8

Veh, vehicle; Ruxo, Ruxolitinib; ND, not determined.
[a]Activation of STAT3 and SMDA2 transcription factors induced in fibroblasts by tumor cell CM was assessed by western blot. Detectable (+) or undetectable (–) phosphorylation.
[b]Contractility and proinvasive activities induced in fibroblasts by tumor cell CM were determined using three-dimensional collagen lattices and organotypic invasion assays. Induction (+); no induction (–).
[c]LIF was detected by ELISA.
[d]LIF and TGF-β blocking antibodies were used either at 10 μg/ml or as stated.

expression (Figure 4C), whereas 67NR CM failed to activate SMAD2 and STAT3 and to induce α-SMA expression (Figure 4C). In vivo, α-SMA expression was detected within the tumor mass of 410.4 tumor microenvironment but not within 67NR tumor, suggesting a strong correlation between the in vitro and in vivo situations (Figures 4Be and f). In tumors, collagen fibers are indicative of a dense ECM and correlate with the invasive potential of tumor cells (Levental et al., 2009; Paszek et al., 2005; Samuel et al., 2011). Assessment of collagen production (Figures 4Bg and h) and collagen fibers assembly (Figures 4Bi–j) in xenograft tumors by Sirius Red staining disclosed enhanced decoration in 410.4 tumors compared with 67NR tumors, with formation of polarized collagen fibers (Figures 4Bi and j and 4D).

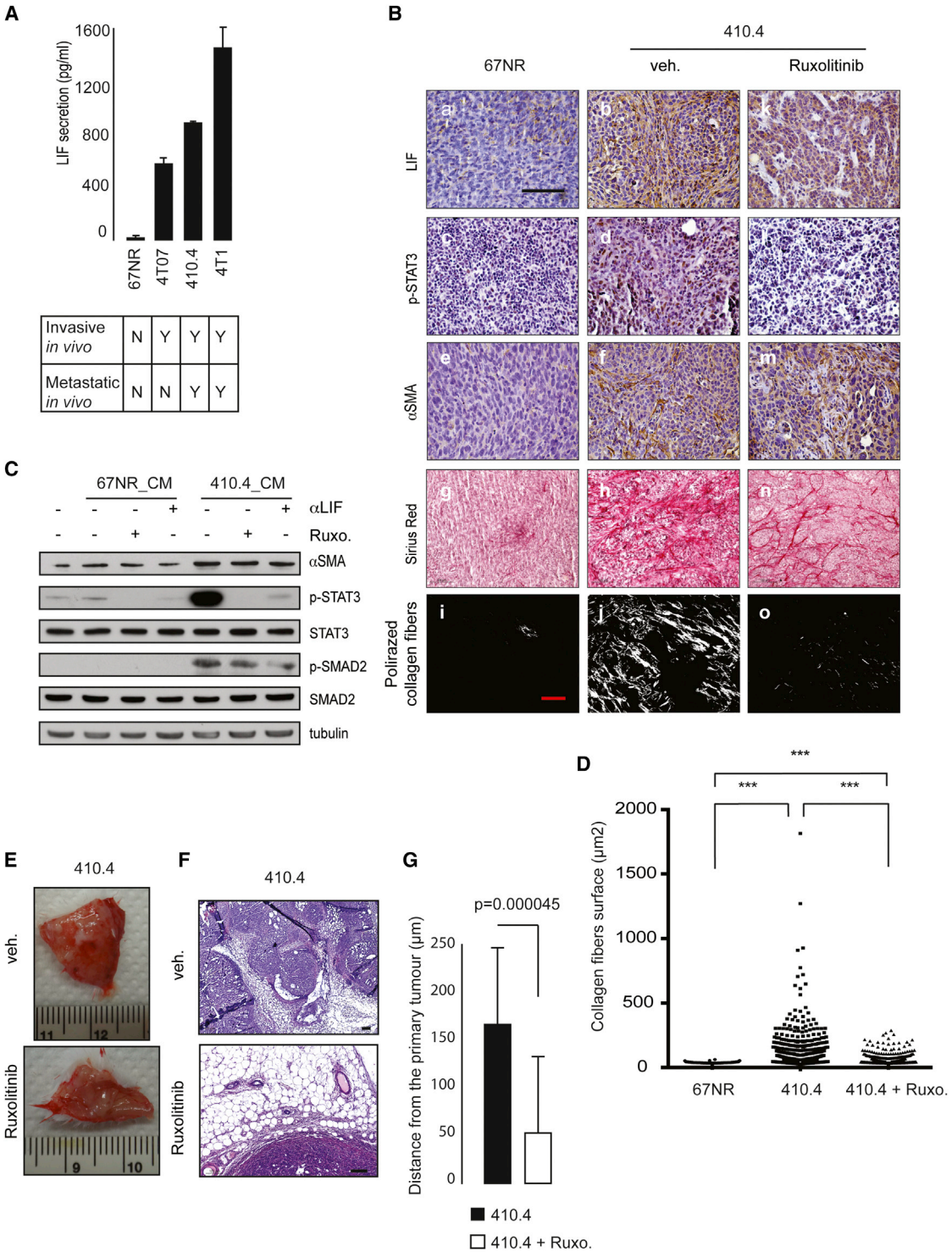

Figure 4. LIF and JAK Signaling Mediate Malignant Tumor Microenvironment In Vivo

(A) ELISA quantification of LIF secreted in mouse breast cancer cells culture media. (UD, undetectable; n = 3 in duplicates). Bottom panel shows the cell invasion and metastatic capacities (Y, yes; N, no).

(B) Immunohistological staining of LIF, p-STAT3, α-SMA, Sirius Red (scale bar, 100 μm), and polarized collagen fibers (scale bar, 50 μm) in orthotopic 67NR and 410.4 mouse breast cancer models 30 days after injection.

(legend continued on next page)

To disclose the fundamental role of JAK kinase activity in fibroblasts-mediated proinvasive ECM remodeling, we further assessed the effect of the JAK1/2 inhibitor Ruxolitinib on tumor microenvironment development in vivo by 21 day oral gavage of mice implanted with 410.4 cells. The drug inhibited STAT3 phosphorylation both within the tumor microenvironment in vivo (Figure 4Bl) and in vitro (Figure 4C), without influencing LIF production (Figure 4Bk) or α-SMA staining (Figure 4Bm). JAK signaling inhibition reduced Sirius Red staining (Figure 4Bn) and formation of collagen bundles (Figures 4Bo and 4D), which underscores the role of JAK in collagen fibers assembly within the tumor microenvironment in vivo, with no detectable incidence of Ruxolitinib treatment on tumor size in vivo (Figure 4E) and 410.4 cells proliferation in vitro (Figure S4B). Consistent with the fact that matrix stiffness promotes tumor cell invasion in vitro and in vivo (Goetz et al., 2011; Levental et al., 2009; Paszek et al., 2005; Provenzano et al., 2008), we disclosed that in mice treated with Ruxolitinib the tumor cells displayed a significant reduced rates of invasion (Figures 4F and 4G).

We next unveiled the collaborative role of both TGF-β and JAK/ROCK signaling during ECM remodeling in vitro. In hDF, and opposite to LIF stimulation (Figure S4Ca–d), fibronectin expression pattern was upregulated by TGF-β1 stimulation (Figures S4Ce and f) and slightly reduced after addition of P6 inhibitor (Figures S4Cg and h). Moreover, TGF-β1-stimulated hDF exhibited an enhanced fibronectin secretion and deposition into the matrix compared to LIF-stimulated and control hDF (Figure S4D). Further, JAK inhibition was ineffective on fibronectin secretion but dramatically reduced its assembly into the matrix (Figure S4D), whereas forced ROCK activation, in absence of JAK activity, rescued proper fibronectin assembly (Figure S4E). Taken together, these data disclose a collaborative role of TGF-β1 and JAK/ROCK signaling in fibroblast-dependent ECM remodeling and matrix protein assembly. We also demonstrated that TGF-β1-stimulated mouse dermal fibroblasts secrete LIF in the culture media (Figure S4F), which leads to collagen gel contraction in vitro (Figure S4G) and in autocrine activation of STAT3 phosphorylation (Figure S4H). Blockade of JAK kinase activity, by either addition of Ruxolitinib or LIF sequestration using a specific blocking antibody, resulted in both complete abrogation of STAT3 phosphorylation (Figure S4H) and matrix remodeling (Figure S4G). Thus, the mice xenograft breast cancer model demonstrated that LIF, independently of α-SMA expression, supports tumor stroma remodeling and that Ruxolitinib by inhibiting JAK, abrogates the proinvasive crosstalk between tumor and stroma cells both in vitro and in vivo.

LIF Is Overexpressed in Human Carcinomas, which Correlates with Invasive Tumor Microenvironment Formationand Poor Clinical Outcome

Randomized analysis of 117 biopsies from human carcinomas, including skin (n = 17), head and neck (n = 50), and lung (n = 50) carcinomas (Table S2), detected strong diffused LIF staining compared to control immunoglobulin (Ig) G or to skin control tissues where LIF expression is confined to basal keratinocytes (Figures 5A and 5B). Subsequent investigation of tumor-stroma remodeling by Sirius Red staining, and observation under polarized light, disclosed collagen fiber organization in human tumors expressing both high and low LIF levels. Thus LIF upregulation clearly correlated with marked assembly of collagen bundles (Figures 5C, 5D, S5A, and S5B) and significantly poor clinical outcome for patients with head and neck and lung carcinomas (Figures 5E and 5F). Further, correlation between LIF detection, Sirius Red staining and presence of invasion nodules was observed in 100 carcinomas (Figure S5C and S5D). Taken together, these data validate our in vitro evidence linking LIF expression to fibroblast-dependent proinvasive ECM remodeling in cancer.

Ruxolitinib Is a Potent Inhibitor of Proinvasive Tumor Microenvironment Remodeling

To confirm the results obtained with mice, the inhibitory effect of Ruxolitinib on collective carcinoma cell invasion was assessed in vitro. The drug (5–10 μM) prevented track formation and SCC12 cell invasion promoted by hCAF (Figures 6A–6C) by inhibiting the CAF endogenous STAT3 activity (Figure 6D). Moreover, Ruxolitinib completely inhibited both TGF-β1- and LIF-dependent activation of hDF contractility in collagen-rich lattices (Figure S6A) and also abrogated proinvasive hDF activation induced upon TGF-β1 and LIF stimulation (Figures S6B and S6C) by repressing STAT3 phosphorylation in TGF-β1- or LIF-stimulated fibroblasts with no effect on SMAD2 (Figure S6D). Because part of the Cyt387 JAK inhibitor effects (Figure S1D) may be due to direct ROCK2 inhibition (Pardanani et al., 2009), we specifically assessed whether effects of Ruxolitinib could be mediated by inhibition of ROCK activity. Forced expression of an active form of ROCK (ROCK-ER) (Croft and Olson, 2006) following 4-hydroxytamoxifen (4OHT) treatment induced MLC2 phosphorylation (Figure S6E) and SCC12 cells invasion (Figure S6F) regardless of Ruxolitinib treatment. However, specific ROCK inhibitors treatment following 4OHT abrogated both SCC12 cell invasion (Figure S6F) and MLC2 phosphorylation (data not shown), therefore, excluding the possibility of nonspecific activity of Ruxolitinib on ROCK activity. Therefore, use of the

(C) Immunoblotting of α-SMA, p-STAT3, and p-SMAD2 in mouse dermal fibroblast long-term stimulated (7 days) using 67NR and 410.4 CM in the absence or presence of LIF blocking antibody and Ruxolitinib inhibitor at 10 μg/ml or 10 μM final concentration, respectively. Immunoblotting of total STAT3, SMAD2, and tubulin as controls.

(D) Quantification of collagen bundles surface (thickness × length in μm^2) shown in Bi, j, and o (each dot represents one fibers). Total quantified fibers: 67NR = 96, 410.4 = 680, and 410.4 + Ruxo = 390.

(E) Representative images of 410.4 orthotopic tumors following Ruxolitinib treatment showing tumor within the mammary fat pad.

(F) H&E coloration of paraffin-embedded sections of 410.4 orthotopic tumors following Ruxolitinib treatment showing tumor cells invasion within the mammary fat pad adjacent the tumor mass. Scale bar, 125 μm.

(G) Quantification of tumor invasion shown in (E). Distance was calculated using ImageJ software by the mean of five measurements from 18 pictures for each condition (mean ± SD; p = 0.000045).

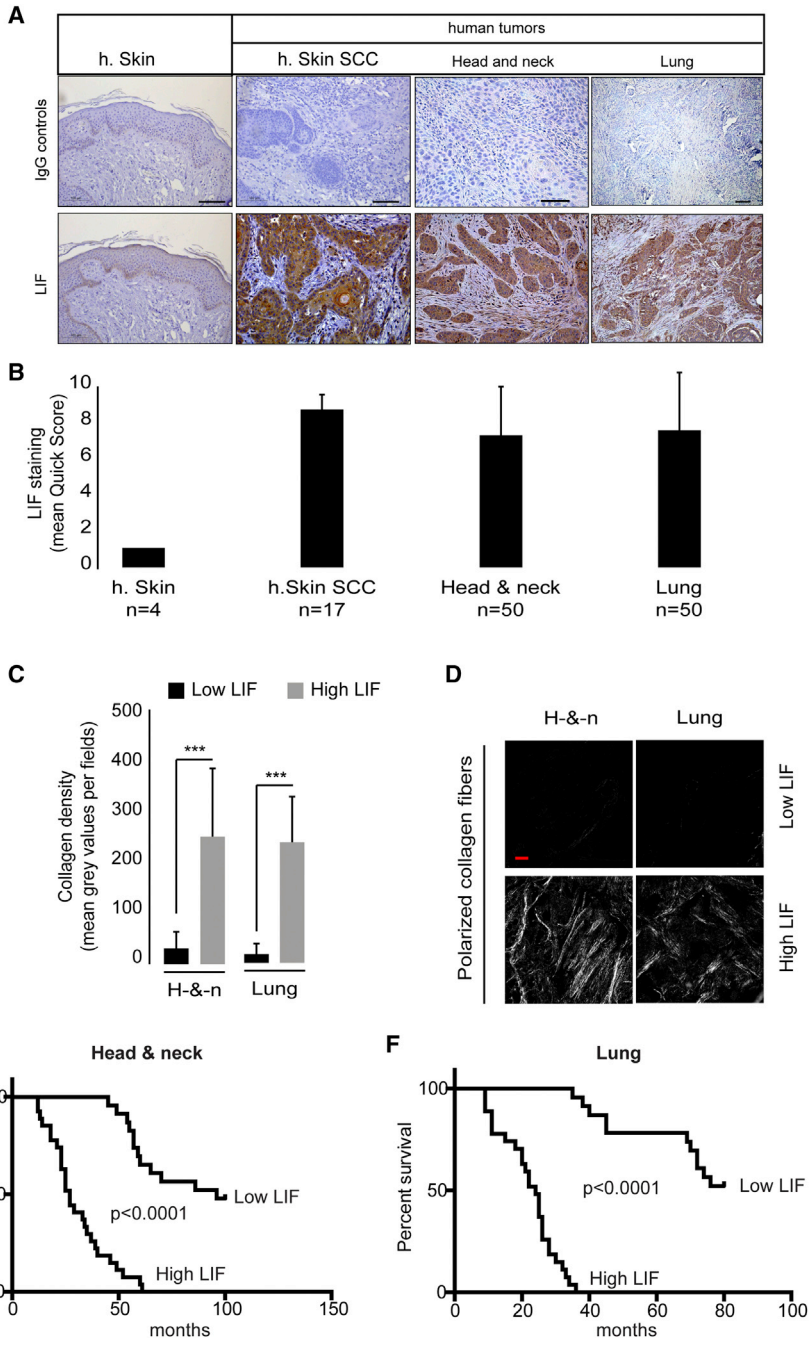

Figure 5. LIF Overexpression in Human Skin SCC Tumors Correlates with Assembled Collagen Fiber Organization

(A) LIF immunohistological staining in human normal skin (h. Skin) and carcinomas from multiple origins (h. Skin SCC tumor n = 17; head and neck carcinomas n = 50 and lung carcinomas n = 50). IgG staining as control. Scale bar, 100 μm.

(B) Quantification of mean Quick Score from tumors shown in (A).

(C) Quantification of collagen fibers density in tumors expressing low and high LIF levels in head and neck and lung carcinomas (mean ± SD of three pictures from ten independent tumors per condition, ***$p < 0.001$).

(D) Sirius Red collagen bundles observed under polarized light in tumors expressing low and high LIF levels quantified in (C). Scale bar, 100 μm.

(E) Kaplan-Meier survival over time of patients with head and neck carcinomas expressing low (n = 23) and high (n = 27) LIF levels.

(F) Kaplan-Meier survival over time of patients with lung carcinomas expressing low (n = 23) and high (n = 27) LIF levels.

JAK1/2 kinase inhibitor Ruxolitinib may pave the way to therapeutic approaches aiming at thwarting not only cancer invasion, but also stroma activation during the early steps of aggressive carcinoma development. To this respect, collagen bundle formation by hDF was verified in vitro using 3D-organotypic cultures. hDF stimulated by either TGF-β1 or LIF showed an enhanced capacity to assembly polarized collagen fibers, which was inhibited by Ruxolitinib (Figures 6E and 6F), which provides further evidence for the role of fibroblast JAK kinase in tumor ECM remodeling.

DISCUSSION

We identify LIF, a member of the IL-6 proinflammatory cytokine family, as the main driver of proinvasive TGF-β-dependent evolution of the tumor microenvironment. LIF mediates autocrine TGF-β1-dependent proinvasive activation in fibroblasts, whereas, in a paracrine manner, tumor-secreted LIF promotes and sustains proinvasive conversion of fibroblast independent of α-SMA expression. LIF is overexpressed in a variety of solid tumors including skin cancers (García-Tuñón et al., 2008; Wysoczynski et al., 2007) and LIF production by tumor cells correlates with their invasive potential (Aslakson and Miller, 1992; Clark et al., 2000). However, downregulation of *LIFr* recently reported in cancer cells (Chen et al., 2012) prompted the idea that tumor cell-derived LIF may exert paracrine effect in tumorigenesis. Here, we propose that paracrine activities of LIF are related to stromal fibroblast proinvasive activation. CAFs are key players of cancer-associated inflammatory processes (Erez et al., 2010; Orimo et al., 2005). Secretion of IL-11 upon TGF-β stimulation of CAFs was shown to induce GP130-IL6ST/STAT3 signaling in colorectal cancer, which confers a survival advantage to metastatic cells and leads to increased efficiency of organ colonization (Calon et al., 2012). Our results, showing that TGF-β1-mediated LIF secretion both in tumor cells and fibroblasts, emphasize the action of TGF-β1 as a driver of

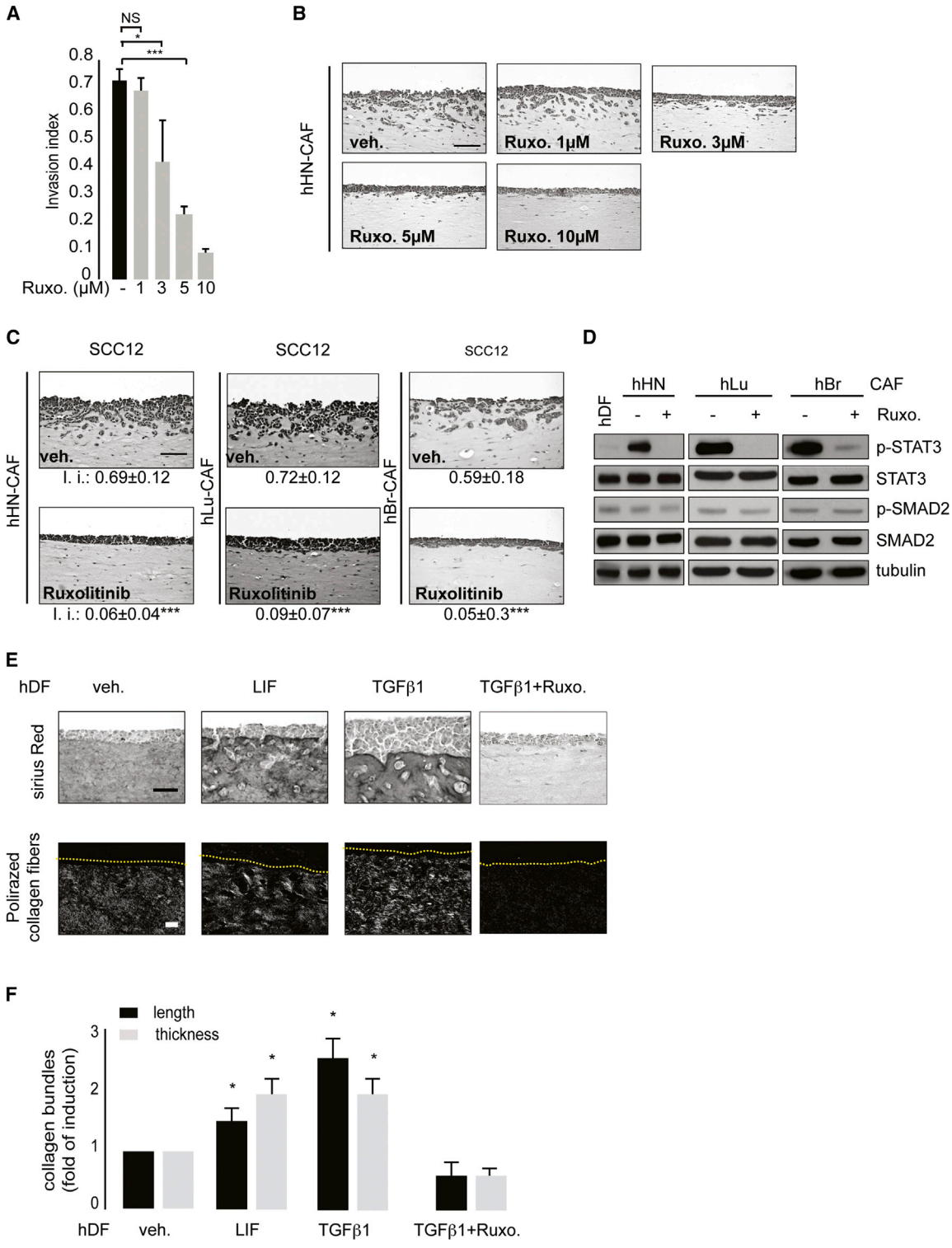

Figure 6. Ruxolitinib Prevents hCAF-Dependent Proinvasive Matrix Remodeling In Vitro

(A) Quantification of SCC12 cells invasion induced by hHN-CAF in presence of Ruxolitinib inhibitor at a stated range concentrations.

(B) H&E coloration of paraffin-embedded sections of SCC12 cells quantified in (A). Scale bar, 100 μm.

(C) H&E coloration of paraffin-embedded sections of SCC12 cells in response to three hCAF (HN, Lu, and Br) in presence or absence (veh.) of 10 μM Ruxolitinib. (I.I., invasion index; n = 3; mean ± SD; ***$p < 0.001$.) Scale bar, 100 μm.

(legend continued on next page)

tumor-associated inflammation, which is a key step for stromal fibroblast proinvasive activation. LIF transcription regulation by TGF-β1 was recently implicated in glioblastoma tumor-initiating cell renewal (Peñuelas et al., 2009), which suggests a general regulation of *LIF* by TGF-β1 in cancer.

α-SMA expression, which is hallmark of CAFs (Kalluri and Zeisberg, 2006), is regulated by TGF-β-dependent signaling (Desmoulière et al., 1993), regulates fibroblasts contractility (Hinz et al., 2001), and correlates with poor clinical outcome in human tumors (Yamashita et al., 2012). Here, we provide evidence that LIF-stimulated dermal fibroblasts, independent of α-SMA expression, promote collagen gel contractility in vitro and that blockade of JAK activity in vivo results in inhibition of tumor-associated collagen network. LIF-activated dermal fibroblasts acquire a contractile phenotype via a crosstalk between the JAK1/STAT3 and RhoA/ROCK/MLC2 signaling pathways, suggesting that α-SMA and Rho-dependent contractility may be regulated by two distinct mechanisms both resulting in cell contractility and ECM remodeling. Within the tumor microenvironment, hCAF are highly heterogeneous, and α-SMA is not expressed by all hCAF cells (Sugimoto et al., 2006). Moreover, PDGFRα has been proposed to be a robust marker for CAFs in a mice model of skin cancer (Erez et al., 2010). Similarly, we noted an increased expression of PDGFRα after LIF stimulation in hPDF (data not shown). In light of our results, we propose that LIF generates subpopulations of CAF cells prone to malignancy independently of α-SMA expression. This may imply that monitoring α-SMA expression is not a criterion sufficient to disclose presence of all the proinvasive fibroblasts within the tumor stroma, which thus may lead to biased favorable prognosis for patients. In contrast, high expression of LIF cytokine in patients with both head and neck or lung carcinomas better correlates with poor clinical prognosis (Figures 5E and 5F).

Actomyosin contractility is crucial for CAF-dependent proinvasive matrix remodeling (Gaggioli et al., 2007). We now provide direct evidence that LIF supports TGF-β1-dependent actomyosin contractility in hPDF. Accordingly, formation of collagen fibers in tumors is indicative of ECM densification and correlates with acquisition of invasive potential by tumor cells (Levental et al., 2009; Paszek et al., 2005; Samuel et al., 2011). Similar to human SCC tumors overexpressing LIF, in vivo orthotopic mouse breast cancer model and hDF in vitro cell cultures disclose that LIF and JAK drive TGF-β1-induced dense collagen fibers remodeling in vivo and in vitro through RhoA and MLC2 overexpression in hDF, which results in increased MLC2 phosphorylation and actomyosin contractility. Actomyosin contractility induces matrix stiffening (Samuel et al., 2011) and, conversely, stiff matrix activates YAP/TAZ and RhoA/ROCK-dependent signaling pathways in CAFs (Calvo et al., 2013) and favors tumor cell invasion (Calvo et al., 2013; Goetz et al., 2011; Levental et al., 2009; Paszek et al., 2005; Provenzano et al., 2008). We now show that forced expression of a constitutively activated ROCK protein is sufficient to induce proinvasive fibroblasts activity in vitro. This loop may constitute a mechanism by which hPDF is also activated during tumorigenesis (Calvo et al., 2013). In this context, TGF-β signaling drives fibronectin extracellular matrix protein expression, whereas JAK1 kinase activity, by regulating actomyosin contractility, is responsible for protein assembly into the matrix, which suggests a collaborative role for both TGF-β and JAK signaling pathways in tumor fibrosis. This finding is in agreement with the fact that JAK2 drives the profibrotic effect of TGF-β signaling in systemic sclerosis and cutaneous fibrosis (Canady et al., 2013; Dees et al., 2012), a process also implying STAT3 in lung fibrosis (O'Donoghue et al., 2012). Because fibrosis is known to be mediated by excessive ECM remodeling and collagen fiber assembly (Wynn and Ramalingam, 2012), it is conceivable that the JAK1/STAT3 signaling route supports the hCAF profibrotic activity in cancer, which results in a matrix prone to collective cancer cell invasion. In light of our data, we propose that, via still undefined mechanisms, constitutive activation of STAT3 may occur in hCAF, which influences invasiveness of human cancers. Accordingly, blockade of JAK activity by the JAK1/2 inhibitor Ruxolitinib counteracts the TGF-β- and LIF-mediated fibroblast-dependent collective carcinoma cell invasion in vitro and in vivo. Ruxolitinib has been approved by the Food and Drug Administration for treatment of patients with intermediate or high-risk myelofibrosis (Mascarenhas and Hoffman, 2012), and this drug is also in a phase II clinical trial for patients with breast or pancreatic cancer in which STAT3 is frequently constitutively activated (Berishaj et al., 2007; Scholz et al., 2003). Therefore, clinical use of the JAK1/2 Ruxolitinib inhibitor may be a promising approach in combination with chemotherapies for patients suffering from aggressive cancers through the targeting of stromal fibroblasts and ECM-associated remodeling events.

In conclusion, our work reveals a novel role of LIF in malignancy. LIF signaling in fibroblasts results in proinvasive tumor microenvironment promotion and mediates TGF-β-dependent fibrosis in cancer. We speculate that blockade of JAK kinase activity within the tumor mass may constitute a promising therapeutic approach to counteract the CAF-dependent protumorigenic ECM remodeling.

EXPERIMENTAL PROCEDURES

Organotypic Invasion Assays

hDF or CAFs cultured during 1 week in serum-free medium (with either vehicle or cytokines) or CM were embedded in matrix gel. Fibroblasts (5×10^5) were embedded in a 1 ml mixture of collagen I and Matrigel (Gaggioli et al., 2007).

Invasion assay was defined by measuring the total areas of SCC cells versus noninvading SCC cells using ImageJ software (http://rsbweb.nih.gov/ij/). The value of invasion index is the average 1 − (noninvading area/total area) of at least ten fields from three or more independent experiments.

(D) Immunoblotting of p-STAT3 and p-SMAD2 in three hCAF (HN, Lu and Br) cells compared to hDF in presence of 10 μM Ruxolitinib. Immunoblots of STAT3, SMAD2, and tubulin shown as controls.

(E) Sirius Red staining of SCC12 cell organotypic invasion assays in presence of hDF control (Veh.) or stimulated by LIF and TGF-β1 in presence or absence of Ruxolitinib. Top and bottom panels show Sirius Red staining under normal and polarized light respectively. Scale bar, 100 μm.

(F) Quantification of thickness and length of collagen bundles shown in (E).

Matrix Remodeling Assay

Fibroblasts (2.5×10^4) were embedded in 100 μl of matrix gel (Hooper et al., 2010). After 1 hr at 37°C, matrices were overlaid with 100 μl serum-free medium (with vehicle or cytokines and/or inhibitors) or CM. Every 2 days, medium was changed, and at day 6 gels were photographed and the respective diameters of the well and gel were measured using ImageJ. The contraction was calculated using the formula 100 × (well diameter – gel diameter)/well diameter.

Orthotopic Tumors in BALB/c Mice

Six- to 8-week-old female BALB/c mice were anesthetized using ketamine and xylazine by peritoneal injection. Skin was incised and 5×10^3 67NR or 410.4 cells were injected into the right and left fourth mammary fat pad in 10 μl of PBS for each mouse. 67NR group consisted of two mice (four primary tumors), 410.4 group of seven mice (14 tumors), and 410.4 with additional treatment of Ruxolitinib (30 mg/kg/day) group of five mice (ten tumors). Mice were sacrificed 30 days postinjection, and Ruxolitinib treatment started 7 days after injection; primary tumors were removed and fixed in PBS containing 3.7% formalin for 8 hr, followed by PBS and transfer to 70% ethanol, and then embedded in paraffin and sectioned and stained with hematoxylin and eosin. Immunohistochemistry detection using anti-LIF, anti-p-STAT3, and anti-alpha-SMA antibodies was performed on paraffin sections following manufacturer's instructions. The protocol was approved by the local ethic committee of the IRCAN institute.

LIF Immunohistological Staining

Formalin-fixed tissues (3.7% in PBS) were transferred to 70% ethanol, embedded in paraffin wax, and sectioned at 7 μm. After deparaffination, microwave antigen retrieval was performed in Na-citrate buffer (10 mM [pH 6] 5 min at 900 W and 25 min at 150 W), and sections were washed in PBS. Endogenous peroxidase activity was then blocked in 1% H2O2 in water for 10 min and sections were washed. After incubation in blocking buffer for 2 hr (10% rabbit serum [S-5000, Vector Laboratories]; 0.3% Triton X-100 in PBS), sections were incubated with LIF primary antibody (#sc-1336, Santa Cruz Biotechnology) diluted 1:50 in blocking buffer overnight at 4°C. For negative controls, rabbit IgG replaced the primary antibody. After three washes in PBS, sections were incubated with biotinylated anti-goat IgG (#BA-5000, Vector Labs) diluted 1:400 in PBS for 30 min and washed in PBS. Samples were processed using Vectastain ABC kit (#PK4001, Vector Labs) and DAB peroxidase substrate kit (#SK4100, Vector Labs) according to manufacturer's instructions. Sections were counterstained with hematoxylin for 5 s, rinsed in water, blued 10 s in 0.08% ammonia water, dehydrated, cleared, and mounted with cover clips.

LIF Staining, Fibrosis, and Tumor Invasion Quantification Method

The protocol was approved by the local ethic committee of the Nice University Hospital. All patients signed an informed consent for inclusion into a research project. All the observations on tumor samples were performed by independent double-blind examiners. The Quick Score (QS) with a 0–16 point scale was used to score the LIF cytokine status within the tumor cells. The QS takes into account both the percentage of positive cells (P, with a 0–4 point scale) and the corresponding staining intensity (I, with a 0–4 point scale) using the formula: $QS = P \times I$. Sirius red staining observed under polarized light was used to score fibrosis within the samples with a 0–4 point scale (0 = no staining; 4 = very strong staining). Fibrosis was quantified on low and high fibrotic samples as determined before by measuring the mean gray value with ImageJ software. Invasion of cancer cells was scored using a 0- to 4-point scale (from 0 = no invasion, to 4 = strong invasion of tumor cells). The number of invasive collective strands and sheets within the stroma was used to score the samples.

Statistical Analysis

Student's t test was performed for quantifications of invasion assay, matrix remodeling assay, ELISA test, and quantitative PCR results (***$p < 0.001$; **$p < 0.01$; *$p < 0.05$).

Kaplan-Meier survival curves were obtained using the PRISM software by comparing two groups of high and low LIF-expressing tumors; p values were obtained using Gehan-Breslow-Wilcoxon test.

SUPPLEMENTAL INFORMATION

Supplemental Information includes Supplemental Experimental Procedures, six figures, and two tables and can be found with this article online at http://dx.doi.org/10.1016/j.celrep.2014.04.036.

AUTHOR CONTRIBUTIONS

J.A. and C.G. designed and performed most of the experiments and analyzed data; I.B. and C.P. performed experiments; V.B. and P.H. provided human carcinomas samples; S.T.-D. provided data for Table 1; C.C.F. designed experiments, performed surgery experiment, and analyzed data from Figure 4; J.A., G.M., and C.G. wrote the paper.

ACKNOWLEDGMENTS

We thank the IRCAN Core Facility for technical assistance in mice, immunohistological, microscopy, and genomic analyses. We thank Mr. E. Selva (Hospital-Integrated Tumor Biobank, Pasteur Hospital, Nice, France) for helping to select the tumor samples. We thank Dr. M. Olson (Beatson Institute, Glasgow, UK), Pr. G. Milano (Centre Antoine Lacassagne, Nice, France), and Dr. T. Magnaldo (IRCAN) for reagents. We thank Drs. E. Sahai, V. Sanz-Moreno, and S. Estrach for critical reading of the manuscript. This work was supported by grants from ARC (RAC12001AAA) and FRM (RAD12004AAA). J.A. is a recipient of an MRT fellowship.

Received: April 17, 2013
Revised: March 27, 2014
Accepted: April 21, 2014
Published: May 22, 2014

REFERENCES

Achyut, B.R., Bader, D.A., Robles, A.I., Wangsa, D., Harris, C.C., Ried, T., and Yang, L. (2013). Inflammation-mediated genetic and epigenetic alterations drive cancer development in the neighboring epithelium upon stromal abrogation of TGF-β signaling. PLoS Genet. *9*, e1003251.

Aslakson, C.J., and Miller, F.R. (1992). Selective events in the metastatic process defined by analysis of the sequential dissemination of subpopulations of a mouse mammary tumor. Cancer Res. *52*, 1399–1405.

Beacham, D.A., and Cukierman, E. (2005). Stromagenesis: the changing face of fibroblastic microenvironments during tumor progression. Semin. Cancer Biol. *15*, 329–341.

Berishaj, M., Gao, S.P., Ahmed, S., Leslie, K., Al-Ahmadie, H., Gerald, W.L., Bornmann, W., and Bromberg, J.F. (2007). Stat3 is tyrosine-phosphorylated through the interleukin-6/glycoprotein 130/Janus kinase pathway in breast cancer. Breast Cancer Res. *9*, R32.

Bhowmick, N.A., Chytil, A., Plieth, D., Gorska, A.E., Dumont, N., Shappell, S., Washington, M.K., Neilson, E.G., and Moses, H.L. (2004a). TGF-beta signaling in fibroblasts modulates the oncogenic potential of adjacent epithelia. Science *303*, 848–851.

Bhowmick, N.A., Neilson, E.G., and Moses, H.L. (2004b). Stromal fibroblasts in cancer initiation and progression. Nature *432*, 332–337.

Boyd, N.F., Guo, H., Martin, L.J., Sun, L., Stone, J., Fishell, E., Jong, R.A., Hislop, G., Chiarelli, A., Minkin, S., and Yaffe, M.J. (2007). Mammographic density and the risk and detection of breast cancer. N. Engl. J. Med. *356*, 227–236.

Calvo, F., and Sahai, E. (2011). Cell communication networks in cancer invasion. Curr. Opin. Cell Biol. *23*, 621–629.

Calon, A., Espinet, E., Palomo-Ponce, S., Tauriello, D.V., Iglesias, M., Céspedes, M.V., Sevillano, M., Nadal, C., Jung, P., Zhang, X.H., et al. (2012). Dependency of colorectal cancer on a TGF-β-driven program in stromal cells for metastasis initiation. Cancer Cell *22*, 571–584.

Calvo, F., Ege, N., Grande-Garcia, A., Hooper, S., Jenkins, R.P., Chaudhry, S.I., Harrington, K., Williamson, P., Moeendarbary, E., Charras, G., and Sahai,

E. (2013). Mechanotransduction and YAP-dependent matrix remodelling is required for the generation and maintenance of cancer-associated fibroblasts. Nat. Cell Biol. *15*, 637–646.

Canady, J., Arndt, S., Karrer, S., and Bosserhoff, A.K. (2013). Increased KGF Expression Promotes Fibroblast Activation in a Double Paracrine Manner Resulting in Cutaneous Fibrosis. J. Invest. Dermatol. *133*, 647–657.

Chen, D., Sun, Y., Wei, Y., Zhang, P., Rezaeian, A.H., Teruya-Feldstein, J., Gupta, S., Liang, H., Lin, H.K., Hung, M.C., and Ma, L. (2012). LIFR is a breast cancer metastasis suppressor upstream of the Hippo-YAP pathway and a prognostic marker. Nat. Med. *18*, 1511–1517.

Clark, E.A., Golub, T.R., Lander, E.S., and Hynes, R.O. (2000). Genomic analysis of metastasis reveals an essential role for RhoC. Nature *406*, 532–535.

Connolly, E.C., Freimuth, J., and Akhurst, R.J. (2012). Complexities of TGF-β targeted cancer therapy. Int. J. Biol. Sci. *8*, 964–978.

Coussens, L.M., and Werb, Z. (2002). Inflammation and cancer. Nature *420*, 860–867.

Croft, D.R., and Olson, M.F. (2006). Conditional regulation of a ROCK-estrogen receptor fusion protein. Methods Enzymol. *406*, 541–553.

De Wever, O., Demetter, P., Mareel, M., and Bracke, M. (2008). Stromal myofibroblasts are drivers of invasive cancer growth. Int. J. Cancer *123*, 2229–2238.

Dees, C., Tomcik, M., Palumbo-Zerr, K., Distler, A., Beyer, C., Lang, V., Horn, A., Zerr, P., Zwerina, J., Gelse, K., et al. (2012). JAK-2 as a novel mediator of the profibrotic effects of transforming growth factor β in systemic sclerosis. Arthritis Rheum. *64*, 3006–3015.

Desmoulière, A., Geinoz, A., Gabbiani, F., and Gabbiani, G. (1993). Transforming growth factor-beta 1 induces alpha-smooth muscle actin expression in granulation tissue myofibroblasts and in quiescent and growing cultured fibroblasts. J. Cell Biol. *122*, 103–111.

Erez, N., Truitt, M., Olson, P., Arron, S.T., and Hanahan, D. (2010). Cancer-associated fibroblasts are activated in incipient neoplasia to orchestrate tumor-promoting inflammation in an NF-kappaB-dependent manner. Cancer Cell *17*, 135–147.

Franco, O.E., Jiang, M., Strand, D.W., Peacock, J., Fernandez, S., Jackson, R.S., 2nd, Revelo, M.P., Bhowmick, N.A., and Hayward, S.W. (2011). Altered TGF-β signaling in a subpopulation of human stromal cells promotes prostatic carcinogenesis. Cancer Res. *71*, 1272–1281.

Gaggioli, C., Hooper, S., Hidalgo-Carcedo, C., Grosse, R., Marshall, J.F., Harrington, K., and Sahai, E. (2007). Fibroblast-led collective invasion of carcinoma cells with differing roles for RhoGTPases in leading and following cells. Nat. Cell Biol. *9*, 1392–1400.

García-Tuñón, I., Ricote, M., Ruiz, A., Fraile, B., Paniagua, R., and Royuela, M. (2008). OSM, LIF, its receptors, and its relationship with the malignance in human breast carcinoma (in situ and in infiltrative). Cancer Invest. *26*, 222–229.

Goetz, J.G., Minguet, S., Navarro-Lérida, I., Lazcano, J.J., Samaniego, R., Calvo, E., Tello, M., Osteso-Ibáñez, T., Pellinen, T., Echarri, A., et al. (2011). Biomechanical remodeling of the microenvironment by stromal caveolin-1 favors tumor invasion and metastasis. Cell *146*, 148–163.

Hanahan, D., and Weinberg, R.A. (2011). Hallmarks of cancer: the next generation. Cell *144*, 646–674.

Hinz, B., Celetta, G., Tomasek, J.J., Gabbiani, G., and Chaponnier, C. (2001). Alpha-smooth muscle actin expression upregulates fibroblast contractile activity. Mol. Biol. Cell *12*, 2730–2741.

Hooper, S., Gaggioli, C., and Sahai, E. (2010). A chemical biology screen reveals a role for Rab21-mediated control of actomyosin contractility in fibroblast-driven cancer invasion. Br. J. Cancer *102*, 392–402.

Joyce, J.A., and Pollard, J.W. (2009). Microenvironmental regulation of metastasis. Nat. Rev. Cancer *9*, 239–252.

Kalluri, R., and Zeisberg, M. (2006). Fibroblasts in cancer. Nat. Rev. Cancer *6*, 392–401.

Kishimoto, T., Akira, S., Narazaki, M., and Taga, T. (1995). Interleukin-6 family of cytokines and gp130. Blood *86*, 1243–1254.

Lederle, W., Depner, S., Schnur, S., Obermueller, E., Catone, N., Just, A., Fusenig, N.E., and Mueller, M.M. (2011). IL-6 promotes malignant growth of skin SCCs by regulating a network of autocrine and paracrine cytokines. Int. J. Cancer *128*, 2803–2814.

Levental, K.R., Yu, H., Kass, L., Lakins, J.N., Egeblad, M., Erler, J.T., Fong, S.F., Csiszar, K., Giaccia, A., Weninger, W., et al. (2009). Matrix crosslinking forces tumor progression by enhancing integrin signaling. Cell *139*, 891–906.

Lin, X.D., Chen, S.Q., Qi, Y.L., Zhu, J.W., Tang, Y., and Lin, J.Y. (2012). Overexpression of thrombospondin-1 in stromal myofibroblasts is associated with tumor growth and nodal metastasis in gastric carcinoma. J. Surg. Oncol. *106*, 94–100.

Mascarenhas, J., and Hoffman, R. (2012). Ruxolitinib: the first FDA approved therapy for the treatment of myelofibrosis. Clin. Cancer Res. *18*, 3008–3014.

Mordasky Markell, L., Pérez-Lorenzo, R., Masiuk, K.E., Kennett, M.J., and Glick, A.B. (2010). Use of a TGFbeta type I receptor inhibitor in mouse skin carcinogenesis reveals a dual role for TGFbeta signaling in tumor promotion and progression. Carcinogenesis *31*, 2127–2135.

Navab, R., Strumpf, D., Bandarchi, B., Zhu, C.Q., Pintilie, M., Ramnarine, V.R., Ibrahimov, E., Radulovich, N., Leung, L., Barczyk, M., et al. (2011). Prognostic gene-expression signature of carcinoma-associated fibroblasts in non-small cell lung cancer. Proc. Natl. Acad. Sci. USA *108*, 7160–7165.

O'Donoghue, R.J., Knight, D.A., Richards, C.D., Prêle, C.M., Lau, H.L., Jarnicki, A.G., Jones, J., Bozinovski, S., Vlahos, R., Thiem, S., et al. (2012). Genetic partitioning of interleukin-6 signalling in mice dissociates Stat3 from Smad3-mediated lung fibrosis. EMBO Mol Med *4*, 939–951.

Olumi, A.F., Grossfeld, G.D., Hayward, S.W., Carroll, P.R., Tlsty, T.D., and Cunha, G.R. (1999). Carcinoma-associated fibroblasts direct tumor progression of initiated human prostatic epithelium. Cancer Res. *59*, 5002–5011.

Orimo, A., Gupta, P.B., Sgroi, D.C., Arenzana-Seisdedos, F., Delaunay, T., Naeem, R., Carey, V.J., Richardson, A.L., and Weinberg, R.A. (2005). Stromal fibroblasts present in invasive human breast carcinomas promote tumor growth and angiogenesis through elevated SDF-1/CXCL12 secretion. Cell *121*, 335–348.

Pardanani, A., Lasho, T., Smith, G., Burns, C.J., Fantino, E., and Tefferi, A. (2009). CYT387, a selective JAK1/JAK2 inhibitor: in vitro assessment of kinase selectivity and preclinical studies using cell lines and primary cells from polycythemia vera patients. Leukemia *23*, 1441–1445.

Paszek, M.J., Zahir, N., Johnson, K.R., Lakins, J.N., Rozenberg, G.I., Gefen, A., Reinhart-King, C.A., Margulies, S.S., Dembo, M., Boettiger, D., et al. (2005). Tensional homeostasis and the malignant phenotype. Cancer Cell *8*, 241–254.

Peñuelas, S., Anido, J., Prieto-Sánchez, R.M., Folch, G., Barba, I., Cuartas, I., García-Dorado, D., Poca, M.A., Sahuquillo, J., Baselga, J., and Seoane, J. (2009). TGF-beta increases glioma-initiating cell self-renewal through the induction of LIF in human glioblastoma. Cancer Cell *15*, 315–327.

Phan, S.H. (2008). Biology of fibroblasts and myofibroblasts. Proc. Am. Thorac. Soc. *5*, 334–337.

Provenzano, P.P., Inman, D.R., Eliceiri, K.W., Knittel, J.G., Yan, L., Rueden, C.T., White, J.G., and Keely, P.J. (2008). Collagen density promotes mammary tumor initiation and progression. BMC Med. *6*, 11.

Samuel, M.S., Lopez, J.I., McGhee, E.J., Croft, D.R., Strachan, D., Timpson, P., Munro, J., Schröder, E., Zhou, J., Brunton, V.G., et al. (2011). Actomyosin-mediated cellular tension drives increased tissue stiffness and β-catenin activation to induce epidermal hyperplasia and tumor growth. Cancer Cell *19*, 776–791.

Sanz-Moreno, V., Gaggioli, C., Yeo, M., Albrengues, J., Wallberg, F., Viros, A., Hooper, S., Mitter, R., Féral, C.C., Cook, M., et al. (2011). ROCK and JAK1 signaling cooperate to control actomyosin contractility in tumor cells and stroma. Cancer Cell *20*, 229–245.

Scholz, A., Heinze, S., Detjen, K.M., Peters, M., Welzel, M., Hauff, P., Schirner, M., Wiedenmann, B., and Rosewicz, S. (2003). Activated signal transducer and

activator of transcription 3 (STAT3) supports the malignant phenotype of human pancreatic cancer. Gastroenterology *125*, 891–905.

Shi, M., Yu, D.H., Chen, Y., Zhao, C.Y., Zhang, J., Liu, Q.H., Ni, C.R., and Zhu, M.H. (2012). Expression of fibroblast activation protein in human pancreatic adenocarcinoma and its clinicopathological significance. World J. Gastroenterol. *18*, 840–846.

Sriuranpong, V., Park, J.I., Amornphimoltham, P., Patel, V., Nelkin, B.D., and Gutkind, J.S. (2003). Epidermal growth factor receptor-independent constitutive activation of STAT3 in head and neck squamous cell carcinoma is mediated by the autocrine/paracrine stimulation of the interleukin 6/gp130 cytokine system. Cancer Res. *63*, 2948–2956.

Sugimoto, H., Mundel, T.M., Kieran, M.W., and Kalluri, R. (2006). Identification of fibroblast heterogeneity in the tumor microenvironment. Cancer Biol. Ther. *5*, 1640–1646.

Szepietowski, J.C., Reich, A., and McKenzie, R.C. (2004). The multifunctional role of leukaemia inhibitory factor in cutaneous biology. Acta Dermatovenerol. Alp. Panonica Adriat. *13*, 125–129.

Takahashi, Y., Ishii, G., Taira, T., Fujii, S., Yanagi, S., Hishida, T., Yoshida, J., Nishimura, M., Nomori, H., Nagai, K., and Ochiai, A. (2011). Fibrous stroma is associated with poorer prognosis in lung squamous cell carcinoma patients. J. Thorac. Oncol. *6*, 1460–1467.

Trimboli, A.J., Cantemir-Stone, C.Z., Li, F., Wallace, J.A., Merchant, A., Creasap, N., Thompson, J.C., Caserta, E., Wang, H., Chong, J.L., et al. (2009). Pten in stromal fibroblasts suppresses mammary epithelial tumours. Nature *461*, 1084–1091.

Wynn, T.A., and Ramalingam, T.R. (2012). Mechanisms of fibrosis: therapeutic translation for fibrotic disease. Nat. Med. *18*, 1028–1040.

Wysoczynski, M., Miekus, K., Jankowski, K., Wanzeck, J., Bertolone, S., Janowska-Wieczorek, A., Ratajczak, J., and Ratajczak, M.Z. (2007). Leukemia inhibitory factor: a newly identified metastatic factor in rhabdomyosarcomas. Cancer Res. *67*, 2131–2140.

Yamashita, M., Ogawa, T., Zhang, X., Hanamura, N., Kashikura, Y., Takamura, M., Yoneda, M., and Shiraishi, T. (2012). Role of stromal myofibroblasts in invasive breast cancer: stromal expression of alpha-smooth muscle actin correlates with worse clinical outcome. Breast Cancer *19*, 170–176.

Yang, J., Mani, S.A., Donaher, J.L., Ramaswamy, S., Itzykson, R.A., Come, C., Savagner, P., Gitelman, I., Richardson, A., and Weinberg, R.A. (2004). Twist, a master regulator of morphogenesis, plays an essential role in tumor metastasis. Cell *117*, 927–939.